10

Optical properties of a-SiC:H/Ag/c-Si composite structure

© K.V. Prigoda, V.O. Bolshakov, S.A. Grudinkin, A.A. Ermina, D.P. Markov, Yu.A. Zharova

Ioffe Institute,
St. Petersburg, Russia

e-mail: piliouguina@mail.ioffe.ru

Received May 04, 2025
Revised June 23, 2025
Accepted October 24, 2025

Optical properties of the composite structure a-SiC:H/hemispherical Ag nanoparticles/c-Si were studied using spectroscopic ellipsometry and reflectometry. Hemispherical Ag nanoparticles on c-Si were obtained by chemical deposition from an $AgNO_3$+HF solution followed by annealing in ambient atmosphere. A layer of a-SiC:H (~ 50 nm) was deposited on the surface of hemispherical Ag particles using plasma-enhanced chemical vapor deposition. A sharp dip to almost zero was observed in the reflectance spectrum with s-polarization in the wavelength range from 701 to 717 nm, the magnitude of which depended on the angle of incidence of light on the sample.

Keywords: hydrogenated amorphous silicon carbide, hemispherical silver nanoparticles, spectroscopic ellipsometry.

DOI: 10.61011/EOS.2025.11.62915.8010-25

Introduction

Films of amorphous silicon carbide (a-SiC) exhibit unique chemical and physical properties, such as a wide bandgap, transparency in the visible range, and thermal and chemical stability [1,2], making them a promising material for various applications in opto- and microelectronic devices [3]. Combining a-SiC with various metals enables the creation of novel composite structures with enhanced characteristics for optoelectronic, photovoltaic [4], plasmonic, and photoluminescent applications [5,6]. For instance, study [7] proposed using Pd/a-SiC composite structures on a porous alumina substrate coated with silver as hydrogen-detecting gas sensors. By combining a-SiC with copper and gold, the authors of work [8] developed nonvolatile resistive memory devices with ultrahigh switching ratios. Meanwhile, [9] introduced the concept of employing multilayer composite structures comprising a-SiC and Ag as high-performance ultraviolet radiation sensors insensitive to visible light. Thus, combining a-SiC with various metals opens new avenues for developing devices with unique physical properties.

The present work reports a study of metal- and hydrogenated amorphous SiC (a-SiC:H) based structures, including the fabrication and optical characterization of such composites using spectroscopic ellipsometry and reflectometry. Silver was selected as the metal due to its high reflectivity and plasmonic properties in the visible spectral range, owing to which silver-containing structures are widely used in diverse fields [10–13]. Moreover, silver is significantly less expensive than other noble metals, rendering devices based on it more cost-effective to produce. The investigated composite structures were fabricated in three stages: 1) formation of an island silver film on the surface of single-crystal silicon (c-Si); 2) thermal annealing of this film to form hemispherical Ag nanoparticles (AgNPs); 3) coating of the nanoparticles on c-Si with a layer of a-SiC:H. Coating the Ag nanoparticles with a-SiC:H enhanced the structure's resistance to external influences and environmental factors. The work examines the features of polarized light reflection from the resulting composite structure in the visible spectral range.

Fabrication of the composite structure

The initial substrate was the c-Si wafer of p-type conductivity with resistivity of $\rho = 1-10\,\Omega\times$cm and (111) crystallographic orientation. An Ag island film was formed on the surface of a clean c-Si wafer by chemical deposition from a $0.02\text{M}\,AgNO_3 + 5\text{M}\,HF$ solution (1:1 ratio) for 30 s. To obtain hemispherical AgNPs, the island film was annealed at 300 °C for 30 min in ambient atmosphere yielding a disordered array of hemispherical AgNPs on c-Si. Subsequently, a layer of amorphous hydrogenated silicon carbide (a-$Si_{1-x}C_x$:H) was deposited onto this array of AgNPs on c-Si by plasma-enhanced chemical vapor deposition from a gas mixture of CH_4, SiH_4 and Ar. The ratio of the carbon- and silicon-containing gas flows was $CH_4/[CH_4 + SiH_4] = 0.8$ roughly corresponding to the film composition with $x = 0.58$. The working pressure in the reactor was 0.1–0.2 Torr, the radiofrequency was 17 MHz, and the radiofrequency power was 0.05 W/cm^2. The resultant structure was a-SiC:H/AgNPs/c-Si with the a-SiC:H layer being ~ 50 nm thick.

Methods of studying the structure

Scanning electron microscopy (SEM)

The morphology of the fabricated composite structure was examined using a JSM-7001F scanning electron mi-

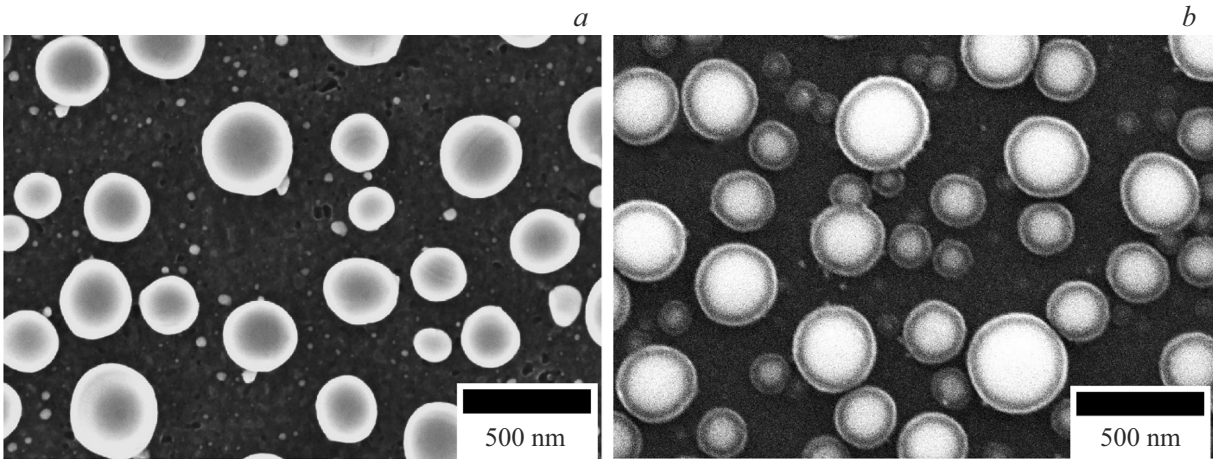

Figure 1. Top-view SEM images of the sample: (a) hemispherical AgNPs on c-Si, (b) hemispherical AgNPs on c-Si after deposition of the a-SiC:H film.

croscope (JEOL, Japan). Measurements were performed in secondary electron mode at an accelerating voltage of 15 kV. SEM image processing enabled statistical analysis of the structure's morphology prior to a-SiC:H layer deposition.

Spectroscopic ellipsometry and reflectometry

The SE-2000 spectroscopic ellipsometer (Semilab, Hungary) was employed to study the optical properties of the structure over a wavelength range of λ from 250 to 900 nm at angles of light incidence of φ from 30° to 79°. Ellipsometric angles Ψ and Δ were measured; these are defined by the fundamental ellipsometry equation:

$$\rho = r_p/r_s = \mathrm{tg}(\Psi)e^{i\Delta}, \qquad (1)$$

where ρ is the relative reflectance of the system, and r_p, r_s are the complex reflectance coefficients for p- and s-polarized light. From Eq.(1), $\Psi = \mathrm{arctg}(|r_p|/r_s|)$, while $\Delta = \arg(r_p/r_s) \equiv \delta r_p - \delta r_s$, where δr_p and δr_s are the phases of the reflected light. Using the SE-2000 ellipsometer, reflection spectra of p- and s-polarized light (R_p and R_s) were also measured for the fabricated structure.

Results and discussion

Structure morphology

Figure 1 shows top-view SEM images of hemispherical AgNPs on c-Si (Fig. 1, a) and the same particles after deposition of the a-SiC:H layer (Fig. 1, b). Statistical analysis of the initial structure—hemispherical AgNPs on c-Si was performed based on top-view SEM images. The silver surface coverage factor on the c-Si substrate was calculated as $f_{\mathrm{Ag}} = 35\,\%$, and the average diameter of the hemispherical AgNPs was determined to be $d_{\mathrm{Ag}} = 161$ nm.

Optical properties of the structure

Figure 2 presents the spectral dependences of ellipsometric angles Ψ and Δ at various angles of light incidence for the a-SiC:H/AgNPs/c-Si structure. The measurement angular range for ellipsometric parameters Ψ and Δ was from 30° to 79° with a step of 5° (except for 79° the maximum angle of the instrument).

Analysis of the spectrum in Fig. 2, a revealed that in the wavelength range 701–717 nm the angle Ψ approaches 90° indicating that r_s tends to zero. The maximum value of the ellipsometric angle Ψ reaching $\sim 89.5°$ was observed at an incidence angle of 68° upon detailed examination of spectra over an angular range of 65°–79° with a 1° step; hence, the dependences for Ψ and Δ (Fig. 2) include spectra at 68° incidence. Also, at a light incidence angle of 68° the spectrum of ellipsometric angle Δ in this range exhibits abrupt behavior (Fig. 2, b): Δ is $-4°$ at 702 nm, $\Delta = 175°$ at 703 nm, and 85° at 704 nm. The values of Δ equal to 270° and $-90°$ are equivalent, as they correspond to the same phase difference between p- and s-polarization vectors.

In the wavelength range 460–482 nm examination of the spectrum in Fig. 2, a showed that the value of angle Ψ decreases and approaches 0° with increasing angle of light incidence (from 30° to 79°). This arises because the amplitude of the p-polarization component exceeds that of the s-component, which is also evident in the reflection spectra: at an incidence angle of 79° R_p approaches 0 (Fig. 3, a). This implies that the reflected light is linearly s-polarized. Meanwhile, the ellipsometric angle Δ at any incidence angle in this spectral range is 180° (Fig. 2, b). As the wavelength increases from 460 to 482 nm, the polarization of the reflected light rotates from right to the left.

Figure 3 shows the reflection coefficient spectra for p- and s-polarized light (R_p and R_s) at light incidence angles from 30° to 79°. Analysis of the spectrum in Fig. 3, a

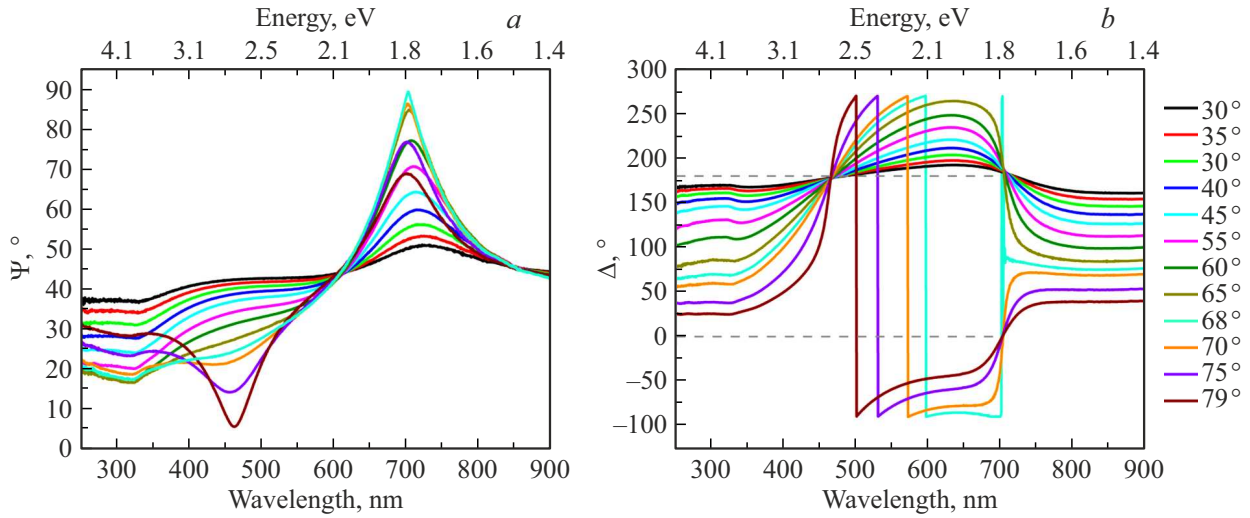

Figure 2. Spectral dependences of ellipsometric angles Ψ (a) and Δ (b) on wavelength at different angles of light incidence for the a-SiC:H/AgNPs/c-Si structure.

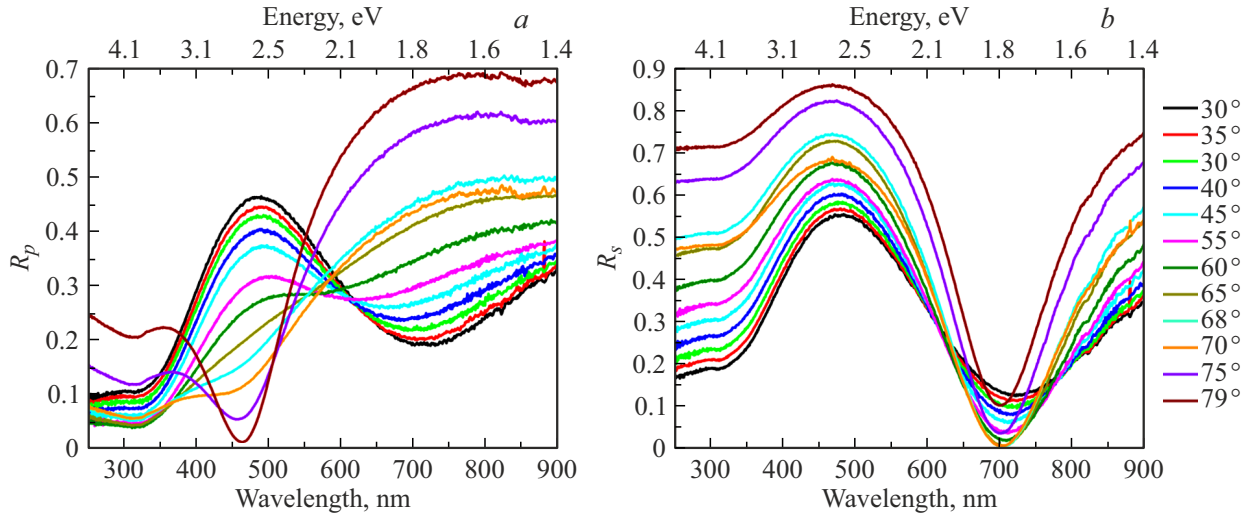

Figure 3. Spectra of reflectance coefficients for p-polarized (a) and s-polarized (b) light at incidence angles from 30° to 79°.

indicated that at incidence angles of 75° and 79° the reflection intensity in p-polarization (R_p) sharply decreases in the 453–462 nm range. Such a narrow dip cannot be attributed to reflection at the Brewster angle, as it would occur over a broad spectral range in that case. Additionally, in the 482–494 nm range, the R_p spectra exhibit a peak at incidence angles from 30° to 55°, while the R_s spectra (Fig. 3, b) show a peak in nearly the same wavelength range at all investigated incidence angles. In the 701–717 nm range R_s tends to 0 (Fig. 3, b), reaching a minimum at a light incidence angle of 68°. Meanwhile, R_p in this range shows a dip at incidence angles from 30° to 45°.

The position and nature of the extrema in the spectral dependences of R_s vary only slightly with incidence angle, so the family of curves can be considered concordant. By contrast, the extrema of R_p match those of R_s at angles below 65° but are opposite at higher angles. A similar optical effect has been observed in metal-dielectric-metal structures [14–16], which exhibit optical anisotropy.

Conclusion

In this work, composite structures of a-SiC:H/AgNPs/c-Si were created, consisting of hemispherical Ag nanoparticles on an c-Si substrate coated with amorphous hydrogenated silicon carbide. The unique optical characteristics and resistance to external influences of the a-SiC:H/AgNPs/c-Si composite structures render them promising for fundamental research and practical applications in fields such as photonics and sensing.

Funding

This work was supported by the Russian Science Foundation (project № 24-22-00334).

Conflict of interest

The authors declare that they have no conflict of interest.

References

[1] V.A. Vasil'ev, A.S. Volkov, E. Musabekov, E.I. Terukov, V.E. Chelnokov, S.V. Chernyshev, Yu.M. Shernyakov. FTP, **24** (4), 710 (1990) (in Russian).
[2] S. Greenhorn, E. Bano, V. Stambouli, K. Zekentes. Materials, **17** (5), 1135 (2024). DOI: 10.3390/ma17051135
[3] M. Barbouche, R. Benabderrahmane Zaghouani, N.E. Ben Ammar et al. J. Mater. Sci.: Mater. Electron., **32**, 20598 (2021). DOI: 10.1007/s10854-021-06570-6
[4] K. Kamakshi, J.P.B. Silva, N.S. Kiran Kumar, K.C. Sekhar, M. Pereira. MRS Commun., **10**, 353 (2020). DOI: 10.1557/mrc.2020.34
[5] K. Kamakshi, K.C. Sekhar, A. Almeida, J. Agostinho Moreira, M.J.M. Gomes. Plasmonics, **10**, 1211 (2015). DOI: 10.1007/s11468-015-9915-4
[6] W. Yu, X.-Z. Wang, W.-L. Dai, W.-B. Lu, Y.-M. Liu, G.-S. Fu. Chin. Phys. B, **22** (5), 057804 (2013). DOI: 10.1088/1674-1056/22/5/057804
[7] A. Sanger, P.K. Jain, Y.K. Mishra, R. Chandra. Sensor. Actuat. B-Chem., **242**, 694 (2017). DOI: 10.1016/j.snb.2016.11.107
[8] L. Zhong, P.A. Reed, R. Huang, C.H. de Groot, L. Jiang. Microelectron. Eng., **119**, 61 (2014). DOI: 10.1016/j.mee.2014.02.004
[9] H. Ferhati, A. Bendjerad, F. Djeffal, A. Benhaya, A. Saidi. *2022 19th International Conference on Electrical Engineering, Computing Science and Automatic Control* (*CCE*) (IEEE, 2022), 1–4. DOI: 10.1109/CCE56709.2022.9975902
[10] O.E. Eremina, N.R. Yarenkov, G.I. Bikbaeva et al. Talanta, **266** (1), 124970 (2024). DOI: 10.1016/j.talanta.2023.124970
[11] A. Tabarov, K. Prigoda, E. Popov et al. Appl. Surf. Sci., **682**, 161771 (2025). DOI: 10.1016/j.apsusc.2024.161771
[12] R. Abbas, J. Luo, X. Qi, A. Naz, I.A. Khan, H. Liu, S. Yu. J. Wei Nanomaterials, **14** (17), 1425 (2024). DOI: 10.3390/nano14171425
[13] F. Alzoubi, W. BaniHani, R. BaniHani, H. Al-Khateeb, M. Al-Qadi, Q. Al Bataineh. J. Clust. Sci., **35**, 2979 (2024). DOI: 10.1007/s10876-024-02708-8
[14] G.E. Lio, A. Ferraro, M. Giocondo, R. Caputo, A. DeLuca. Adv. Optical Mater., **8** (17), 2000487 (2020). DOI: 10.1002/adom.202000487
[15] N. Priscilla, D. Smith, E. Della Gaspera, J. Song, L. Wesemann, T. James, A. Roberts. Adv. Photonics Res., **3** (5), 2100333 (2022). DOI: 10.1002/adpr.202100333
[16] M. Iwanaga. *Plasmonic resonators: fundamentals, advances, and applications* (Pan Stanford Publishing Pte. Ltd., Singapore, 2016), 1st ed. DOI: 10.1201/9781315364711

Translated by J.Savelyeva